THE BEHAVIOUR OF BRICK MASONRY UNDER BIAXIAL STRESS WITH PARTICULAR REFERENCE TO INFILLED FRAMES

M DHANASEKAR Postgraduate Student
A W PAGE Senior Lecturer
P W KLEEMAN Senior Lecturer
Department of Civil Engineering and Surveying, University of Newcastle, N.S.W. Australia

ABSTRACT The results of 180 biaxial tests on half-scale brick masonry panels have been used to establish representative stress-strain relations and a failure surface for solid brick masonry. The results, expressed in stress and strain components related to the jointing planes, are used in the formulation of a finite element model of brick masonry in which non-linear deformations, cracking and sliding of the joints can be taken into account. The model is used to predict the behaviour of three infilled frames under racking loads and is compared with test results on those frames. Good agreement is obtained.

1. INTRODUCTION

Masonry is extensively used as an infill material in framed construction, but its contribution to the strength and stiffness of framed structures is usually neglected in design. The main reason for disregarding the infill lies in the complexity and uncertainties associated with the stress analysis of the infill.

The structural action of infilled frames subjected to racking load may be summarised as follows; at a relatively low load the bounding frame separates from the infill in the "tension" corners and stable contact lengths develop at the diagonally opposite "compression" corners. The extent of the contact lengths depends upon the stiffness of the bounding frame. The diagonal loading of the panel results in zones of high compressive stress near the corners and a non-uniform distribution of shear and normal stress on the horizontal jointing planes in the interior of the panel. At substantially higher loads, a shear failure starts near the centre of the panel and progresses towards the loaded and reaction corners. The final failure mode depends upon the relative stiffness of the frame and the infill. In more flexible frames a corner crushing failure is observed whereas stiffer frames are associated with a continuous path of sliding and cracking of the infill.

A number of experiments have been carried out on model and full scale infilled frames by Benjamin and Williams (1), Mainstone (8) and Kadir and Hendry (7) to determine the strength and stiffness of frames with brick masonry infill. The contribution of the infill has been generally found to be significant. From some of these results and further tests of his own, Holmes (6) proposed an "Equivalent Strut Model" for the analysis of infilled frames. Smith (12) expressed the effective width of the equivalent strut as a function of the relative stiffness of the frame and the infill. However, in the analysis to date, only elastic, brittle, isotropic infills have been considered with no allowance for inelastic behaviour or the influence of the jointing planes on failure.

For a realistic stress analysis of infilled frames, the constitutive relations and the failure characteristics of the infill material are required. In this paper the results from 180 biaxial tests on half scale brick masonry panels are summarised and have been used to establish representative stress-strain relations and failure criteria for solid brick masonry. These properties are best expressed in terms of stress and strain components which are related to the jointing

directions of the masonry and are used in formulating an iterative finite element model for the analysis of infilled frames. The adequacy of the stress analysis is assessed by comparing the predicted and observed behaviour of three test frames subjected to racking loads.

2. MATERIAL PROPERTIES OF BRICK MASONRY

The elastic and non-linear stress-strain relations and the failure surface of brick masonry required for a finite element model were derived from the results of a large number of biaxial tests on square panels of the masonry and are summarised below.

A total of 180 panels, each 360 mm square, was tested with the prime purpose of establishing failure criteria for brick masonry under biaxial stresses. The panels were made from half scale solid pressed clay bricks with a cement:lime:sand mortar of proportions 1:1:6 by volume. The joints were 5 mm in thickness, and were orientated at five different angles θ of the bedjoint to the major compressive stress (i.e. $\theta = 0°$, 22.5°, 45°, 67.5° and 90°). The panels were tested under biaxial compression-compression and tension-compression. The load was increased monotonically in all tests, and the ratio of the principal stresses, while fixed for a particular test, varied through the range $\sigma_1/\sigma_2 = \infty$, 10, 4, 2, 1, -0.5, -0.25, -0.10, $-\infty$. In each test average strains on 270 mm gauge lengths were also recorded. Details of the test procedure have been reported elsewhere (9, 10).

2.1 Deformation Characteristics

The experimental strain data (which are averages over several bricks and joints) have been transformed so that they relate to a coordinate system aligned parallel and perpendicular to the bedjoints. Three stress-strain curves were obtained for each test, namely, Normal Stress-Strain ($\sigma_n - \varepsilon_n$), Parallel Stress-Strain ($\sigma_p - \varepsilon_p$) and Shear Stress-Strain ($\tau - \gamma$).

Most of the panels subjected to biaxial compression-compression stress states were found to have distinctly non-linear stress-strain relations, whereas panels subjected to tension-compression stress states had stress-strain relations which were close to linear. For panels with high shear stresses and low normal stresses on the bedjoint, ($\sigma_n/\sigma_p < 0.25$ and $\tau/\sigma_n > 1.0$) initial failure occurred by cracking or sliding along the bedjoint. Although these panels were capable of sustaining higher loads, the failure load was taken to be the load at which the initial failure was observed.

2.1.1 Elastic Properties. It was first assumed that the masonry panels were orthotropic. Elastic constants were determined from a least squares analysis of the initial linear portions of the stress-strain curves. The results suggested that the panels tested were on average close to isotropic in the elastic range, and, upon reanalysis, average values of 5700 MPa for Youngs Modulus and 0.19 for Poisson's Ratio were obtained. Details of the above analysis together with data on the variability of the elastic constants are given in (2).

2.1.2 Non-linear Stress-Strain Relations. For the panels subjected to biaxial compression-compression the stress-strain curves were distinctly non-linear. The "plastic" strains, i.e. those parts of the total strain which remain after subtracting the strains determined by extrapolating the initial slopes of the curves, were found to vary with a power of the stress which ranged from 2 to 6. An initial assumption of isotropic plastic behaviour was found to be unsuitable. Non-isotropic stress-plastic strain relations were then sought. Given the variability of the data, it was found reasonable to assume that each plastic strain component was dependent only on its corresponding stress and that average values of the plastic components of strain were given by;

$$\varepsilon_n^p = 1.42 \times 10^{-6} \sigma_n^{3.3} \quad \ldots\ldots\ldots (1)$$

$$\varepsilon_p^p = 1.05 \times 10^{-6} \sigma_p^{3.3} \quad \ldots\ldots\ldots (2)$$

$$\gamma^p = 62.5 \times 10^{-6} \tau^{4.0} \quad \ldots\ldots\ldots (3)$$

Where ε_n^p, ε_p^p, γ^p are the Normal, Parallel and Shear plastic strains and σ_n, σ_p, τ are the corresponding stresses.

The non-linear stress-strain relations have been discussed in detail in Reference 3.

2.2 Failure Surface

A three dimensional surface is necessary to define the failure of masonry because the mortar joints act as planes of weakness and the orientation θ of those planes influences the failure mode. Each test provided a failure stress point in the (σ_1, σ_2, θ) space. Failure surfaces obtained for the compression-compression and tension-compression quadrants of the (σ_1, σ_2, θ) space have been reported earlier (9, 10). The failure surface in the (σ_1, σ_2, θ) space is not regular in shape and is difficult to express analytically.

The failure stresses were therefore transformed so that they related to coordinate axes normal and parallel to the bedjoints. The failure surface in terms of the stress components σ_n, σ_p and τ was able to be idealized as three intersecting elliptic cones in the σ_n, σ_p, τ space. This idealized surface is shown in Figure 1. It is symmetric with respect to the σ_n-σ_p plane. Each cone may be expressed analytically as

$$C_1\sigma_n^2 + C_2\sigma_p^2 + C_3\tau^2 + C_4\sigma_n\sigma_p + C_5\sigma_n + C_6\sigma_p + 1 = 0 \quad \ldots\ldots\ldots (4)$$

The constants (C_i, i = 1,6) are given for each of the three cones in Table A1. The two end cones correspond approximately with maximum principle tensile and compressive stress criteria for failure. The intermediate cone is for the most part associated with failure under combined shear and normal stress on the joints. Further details of the derivation, and discussion of its limitations, are given in (4).

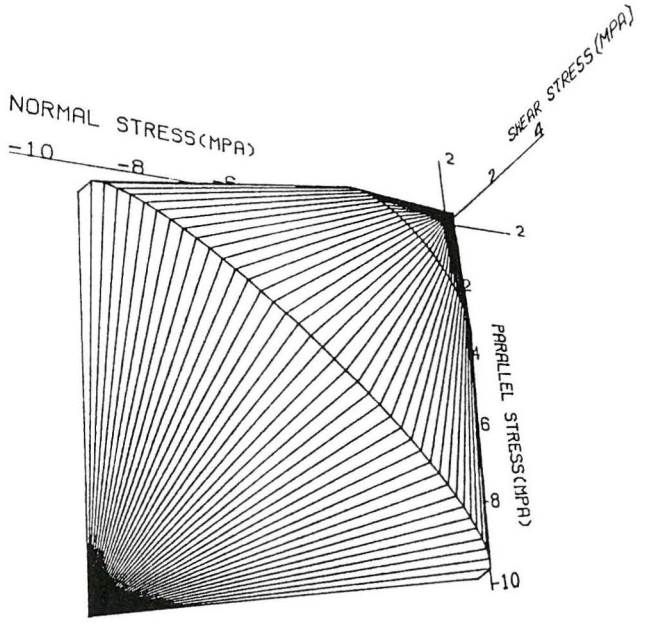

Fig 1 Failure Surface in σ_n, σ_p, τ space

3. FINITE ELEMENT MODEL FOR INFILLED FRAMES

The above stress-strain relations and failure surface have been incorporated into a finite element program for the determination of the displacements and stresses in, and the failure of, infilled frames. The program is able to take account of the non-linear load-deflection behaviour, the separation of the frame from the infill and the post cracking behaviour of the infilled frames. A brief summary of the program is given below but some further details may be found in (5).

3.1 Element Types

The brick masonry infill has been modelled as a continuum using the macroscopic stress-strain relations and failure surface outlined in section 3. It is able to account for the influence of the mortar joints even with a relatively coarse subdivision of the infill area. The frames are assumed to be subjected to in-plane loads, for which plane stress conditions are considered appropriate. Eight noded isoparametric elements with four point Gaussian integration were chosen to allow for moderate stress gradients in the infill.

The mortar joint between the infill and the frame has been modelled using a six noded isoparametric one dimensional joint element. Three point Gaussian integration was used in conjunction with bilinear stress-strain relations in both shear and compression. The initial shear modulus of 600 MPa and Youngs Modulus of 1250 MPa were the same as those determined by Page (11) for a similar mortar. The failure criterion for a joint element under shear and compression was approximated by a bilinear relation between the shear stress and the compressive stress. The tensile bond strength of the joint between the steel frame and the mortar was low and therefore assumed to be zero.

The frame has been modelled using conventional two noded beam elements with three degrees of freedom at each node. To account for the eccentricity between the centre line of the frame and the outer edge of the mortar joint, the stiffness matrix of the beam element was transformed to suit displacements at the beam-joint interface. The beam element was assumed to remain elastic.

3.2 Program Structure

In the program, loads are applied incrementally, with two iterative loops at each load level, one to allow for the material non-linearity and the other to allow cracking to progress. The stresses at Gauss points in each element at which the stress state is biaxial compression-compression are evaluated using incremental relations based on equations (1), (2) and (3). At other Gauss points the material is assumed to be linearly elastic up to failure.

At a given load level, iteration continues until the unbalanced nodal forces associated with material non-linearities are less than a chosen tolerance. The stresses are then checked for violation of the failure surface. If failure is indicated in an element, the stress-strain matrix is modified by reducing the appropriate tangent modulus to approximately 5% of its original value. With tension cracks, a crack is simulated by introducing opposing forces which cancel the previously existing stresses. For shear failure in joints in which the direct stress is compression, frictional shear stresses are maintained.

When modelling a racking test on an infilled frame, failure takes place at progressively more Gauss points in the infill, and the overall deflection of the frame increases rapidly. Eventually a load level is reached at which the slope of the load-deflection curve is close to that of the bare frame. (Note that even

when the shear failure has progressed across the whole panel, appreciable frictional shear stresses remain on the joint failure planes.)

4. VERIFICATION TESTS ON INFILLED FRAMES

Several infilled frames have been tested to verify the finite element model discussed in the previous section. The results of three of the tests are outlined below and compared with the results given by the finite element analyses of the frames.

4.1 The Test Frames

One rectangular and two square infilled frames were made. Two cold formed steel channel sections were welded back to back to form an I section of depth 51 mm and flange width of 50 mm. The section was used in the rectangular frame and one of the square frames.

The second square frame was built with tapered flange I section members of depth 127 mm and flange width of 64 mm. Additional 8 mm plates were used as web stiffeners at the loaded and reaction corners. The centre to centre dimensions of the framing members are given in Table A2. Also given in the table is the parameter λh which measures the ratio of the stiffness of the infill to the stiffness of the frame. It is defined by

$$\lambda h = h. \left(\frac{E_b \ t \sin 2\theta}{4 \ E_s \ I \ h} \right)^{\frac{1}{4}} \qquad \ldots\ldots\ldots (5)$$

in which E_b, t and h are Youngs Modulus, thickness and height of the brick masonry infill respectively; E_s and I are the Youngs Modulus and second moment of area of the column and θ is the slope of the infill diagonal to the horizontal.

To minimise workmanship problems, the infill was constructed within the frame whilst in a horizontal position. The mortar was then poured in to the vertical joints and vibrated gently to remove the air bubbles. All bed and head joints were 5 mm with an 8 mm joint between the infill and the frame. Each panel was moist cured for 28 days.

4.2 Instrumentation

Electrical resistance strain gauges were attached to the steel frames at sufficient points to allow bending moments and axial forces to be determined at a number of sections. Targets for demountable (Demec) extensometers were glued to the brick masonry infill in 45° rosette arrays at a number of locations. The extensometer gauge length of 200 mm was sufficient to extend across at least one mortar joint horizontally and several joints vertically. Deflection measurements were taken with mechanical dial gauges around the outside of the frame.

4.3 Testing

All three infilled frames were tested under monotonically increasing racking load until the brick masonry infill failed. The load was applied horizontally near the top of one of the frame verticals and reacted at a horizontal support near the bottom of the other vertical. In-plane rotation of the frame was prevented by roller supports at the top of the first vertical and the bottom of the second. The load was increased in 5 kN increments until a continuous crack across the panel was readily visible.

5. COMPARISON OF RESULTS

The intention in carrying out the tests on the infilled frames was to verify the accuracy of the finite element model and not to draw extensive conclusions about the general behaviour of infilled frames. Once the model has been verified, a parametric study of frame behaviour can be carried out. Such a study forms a later stage of this research program.

A comparison of the test results of the three infilled frames with the results of the corresponding finite element analyses is given in Figures 2, 3, 4 and 5. Agreement between the two sets of results is generally good. In particular, the load levels at which the brick masonry infills fail, and the overall load-deflection curves, show excellent agreement. Differences in local behaviour in the frame or infill can be expected to be more sensitive to modelling errors and these are discussed in detail below.

5.1 The Load-Deflection Behaviour

The results for the two frames with $\lambda h = 6.34$ and $\lambda h = 6.44$ show that while λh is a useful indicator of relative stiffness, it is insufficient by itself to characterise the strength of the infill if the geometrical proportions of the panel change. This agrees with the conclusions of Smith and Carter (12). A comparison of the results of the two square frames shows that the infill of the stiffer frame carries a load which, at a lateral displacement of 1.2 mm, is some 33% greater than the load in the weaker frame. This may be attributed to the greater contact lengths and hence greater effective width of the "equivalent strut" in the stiffer infilled frame (12).

After the initial failure of the infill the stiffness of each infilled frame approaches that of the corresponding bare frame, but it should be noted that the infill continues to resist a proportion of the lateral load by frictional shear on the planes of failure.

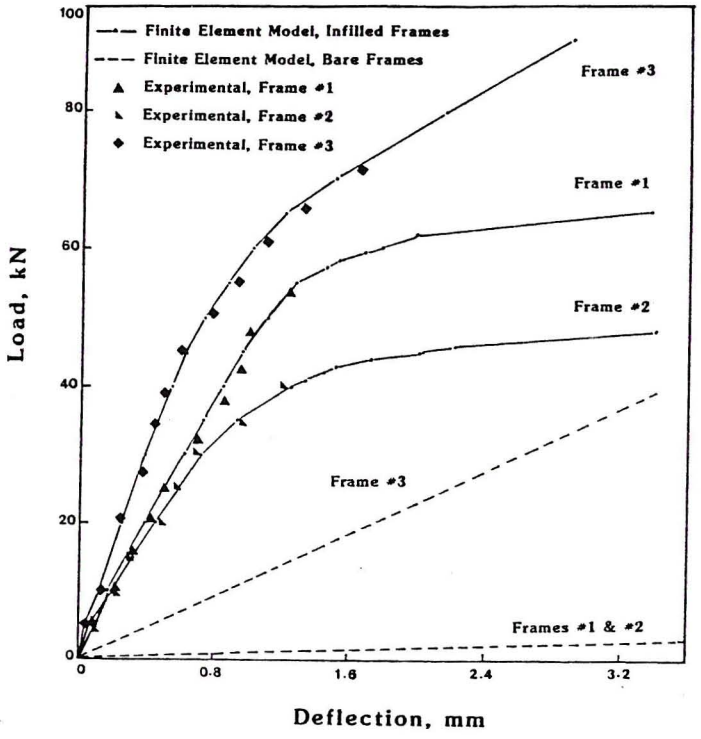

Fig 2 Load-Deflection Curves for the Infilled Frames

5.2 Variation of the Bending Moment with Load

The bending moment in the frame is affected by the separation of the frame and infill. The variation of bending moment with applied load at two sections in the column, one near the loading point and the other near the "tension corner", is plotted for the rectangular frame and a square frame in Figures 3(a) and 3(b) respectively. Both finite element and experimental results are shown.

Effects which influence the bending moments include the separation of the frame and infill, the non-linear deformation of the infill and extent of cracking and sliding in the joints. Given the variability of each of these effects, the agreement between the finite element model and the test results is satisfactory.

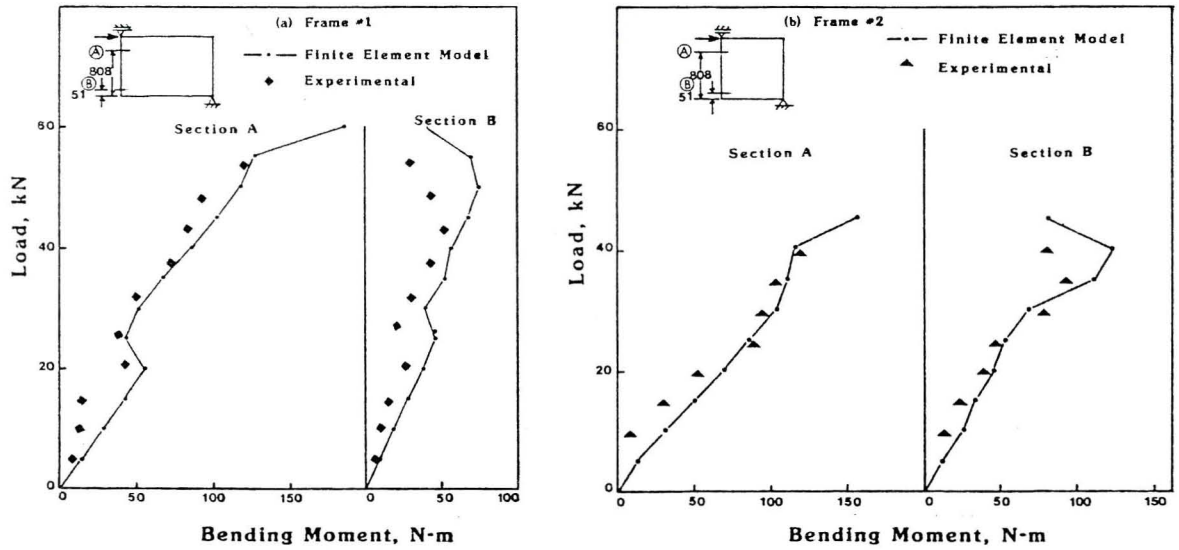

Fig 3 Variation of Bending Moment with Load

5.3 The Bending Moment Diagrams

The bending moment diagrams for each of the frames at load levels of 25 kN are shown in Figures 4(a) and 4(b). Experimentally determined bending moments are also shown. Experimental values of bending moment at the corners could not be obtained because of the difficulties in measuring strains in the stiffened corners. The two sets of moments are generally in good agreement. There is a suggestion that for the square frame, the experimental contact length along the bottom beam was greater than the calculated length.

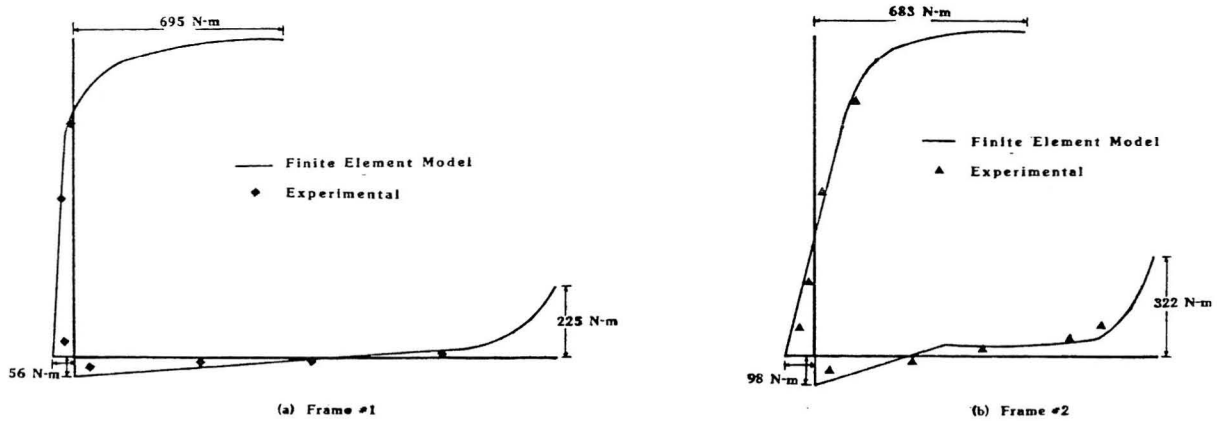

Fig 4 Bending Moment Diagrams for the Beam and Column at 25 kN Load

5.4 Variation of the State of Strain near the Loaded Corner

The strains at a point in the brick masonry infill depends on the length of contact between the frame and the infill. This in turn is dependent upon the relative stiffness of the frame and the infill, and, to a lesser extent, the shear strength of the joint between the frame and the infill. The predicted and measured load-strain curves of panels 1 and 2 are plotted in Figures 5(a) and 5(b) respectively. The agreement between the results of the finite element model and the experiment is again satisfactory, especially in view of the local variability which is possible in the properties of the brick masonry infill.

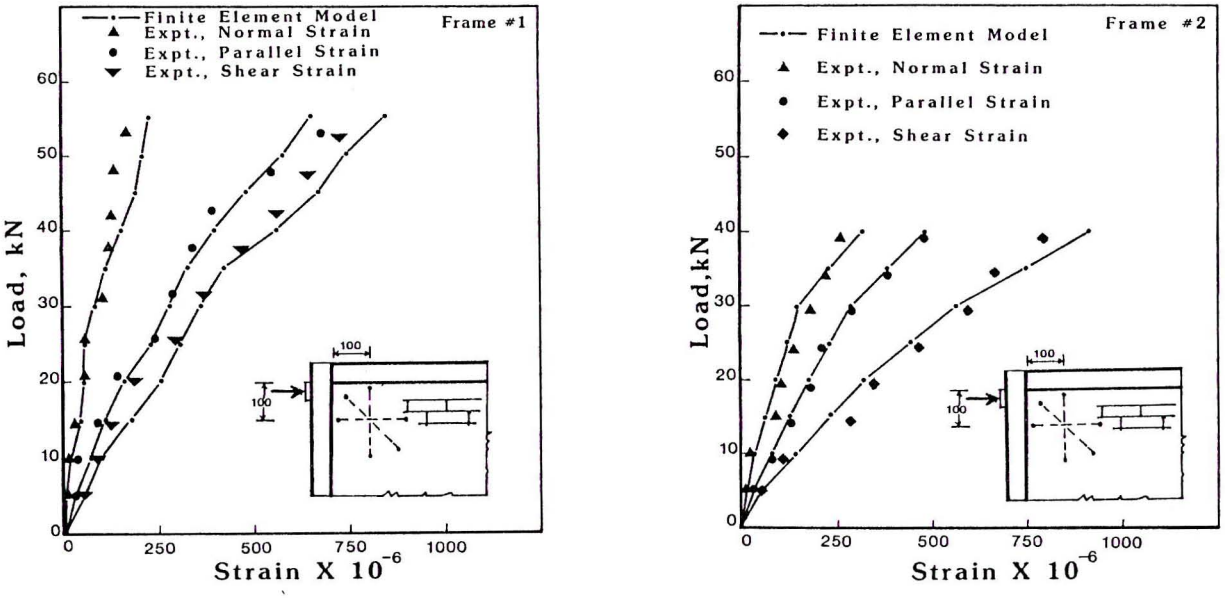

Fig 5 Variation of Strains near to Loaded Corner

5.5 Failure Load of the Brick Masonry Infill

The cracks in the brick masonry infill in the three panels tested were visible to the naked eye at loads of 55.5 kN, 45 kN and 65 kN. The finite element model predicted the formation of a continuous crack across the panel at 57 kN, 43 kN and at 61 kN respectively. The agreement between the test results and the finite element model is again satisfactory.

6. CONCLUSIONS

The results from 180 biaxial tests on half scale brick masonry panels have been used to establish representative stress-strain relations and failure criteria for solid brick masonry. These properties are best expressed in terms of stress and strain components which are related to the jointing directions of the masonry and are used in formulating an iterative finite element analysis of brick masonry. This incremental load model is able to reproduce the non-linear behaviour caused by material non-linearity and by progressive cracking and sliding. Crushing failures in localised areas are also predicted. The material properties required for other types of brick masonry may be obtained from a limited set of tests on brick masonry panels but some biaxial tests are still necessary.

The adequacy of the finite element model is checked by comparison of its results

with the experimental results from racking tests on three steel frames with brick masonry infill. The frames were loaded until a continuous crack had progressed across the brick masonry. The load-deflection curves and the loads at which the crack is completely formed are in excellent agreement. Results which can be expected to be more sensitive to modelling errors such as the variation with load of bending moment at sections in the frame, the variation of bending moment around the frame and the variation with load of the strains near the loaded corner are also in good agreement. The finite element model can therefore be used in parametric studies of brick masonry infilled frames with some confidence.

The finite element analyses and test results confirm earlier conclusions drawn for isotropic infill materials, namely, that

(a) separation of the infill and the frame takes place at low load levels,
(b) the relative stiffness parameter λh is insufficient by itself to characterise the strength of the infill as the proportions of the frame change,
(c) the infill in stiffer frames carries a higher load before failure, that is, the effective width of the "equivalent strut" is increased,
(d) the infill is capable of sustaining load by frictional shear even after a continuous crack has progressed across the infill.

7. ACKNOWLEDGEMENTS

The assistance of Mr. L. McLardy, Senior Craftsman, and other Laboratory Staff of the Department of Civil Engineering and Surveying, the University of Newcastle is gratefully acknowledged. Part of the research is financed by the Australian Research Grants Scheme. Bricks were supplied by PGH Ceramics-Bricks, N.S.W.

8. REFERENCES

(1) BENJAMIN, J.R. and WILLIAMS, H.A. "The Behaviour of One Storey Brick Shear Walls". *Journal of Structural Division, ASCE*, Vol. 84, No ST4, pp 1723.1-1723.30, 1958.

(2) DHANASEKAR, M., PAGE, A.W. and KLEEMAN, P.W. "The Elastic Properties of Brick Masonry". *International Journal of Masonry Construction*, Vol. 2, No 4, pp 155-160, 1982.

(3) DHANASEKAR, M., KLEEMAN, P.W. and PAGE, A.W. "Biaxial Stress-Strain Relationships for Brick Masonry". *Journal of Structural Engineering, ASCE*, 1984 (in Press).

(4) DHANASEKAR, M., PAGE, A.W. and KLEEMAN, P.W. "The Failure of Brick Masonry Under Biaxial Stresses". Submitted for publication to the *Proceedings, Institution of Civil Engineers*, Part II, United Kingdom, 1985.

(5) DHANASEKAR, M., PAGE, A.W. and KLEEMAN, P.W. "A Finite Element Model for the In-Plane Behaviour of Brick Masonry". *Ninth Australasian Conference on the Mechanics of Structures and Materials*, University of Sydney, pp 262-267, 1984.

(6) HOLMES, M. "Steel Frames with Brickwork and Concrete Filling". *Proceedings, Institution of Civil Engineers*, Vol. 19, pp 473-478, 1961.

(7) KADIR, M.R. and HENDRY, A.W. "The Behaviour of Brickwork Infilled Frames Under Racking Load". *Proceedings, British Ceramic Society*, Load Bearing Brickwork (5), No 24, pp 65-77, 1975.

(8) MAINSTONE, R.J. "On the Stiffness and Strength of Infilled Frames". *Proceedings, Institution of Civil Engineers*, Supplement (iv), Paper 7360S, pp 57-90, 1971.

(9) PAGE, A.W. "The Biaxial Compressive Strength of Brick Masonry". *Proceedings, Institution of Civil Engineers*, Part II, Vol. 71, pp 893-906, 1981.

(10) PAGE, A.W. "An Experimental Investigation of the Biaxial Strength of Brick Masonry". *Proceedings, Sixth International Brick Masonry Conference*, pp 3-15, Rome, 1982.

(11) PAGE, A.W. "A Finite Element Model for Masonry". *Journal of Structures Division, ASCE*, Vol. 104, No ST8, pp 1267-1285, 1978.

(12) SMITH, B.S. and CARTER, C. "A Method of Analysis of Infilled Frames". *Proceedings, Institution of Civil Engineers*, Part II, Vol. 44, pp 31-48, 1969.

APPENDIX A

TABLE A1 Constants of the Failure Surfaces

Cone	C_1*	C_2*	C_3*	C_4*	C_5*	C_6*
1	0.060	-0.640	-24.3	12	119	95.8
2	-262	-327	-3260	2720	-1860	-1110
3	-29.4	-34.0	-6150	5960	-2660	-2080

* constants are multiples of 10^3

TABLE A2 Details of the Infilled Frames Tested

Frame	Length (mm)*	Height (mm)*	Frame Section (mm)	λh
1	1555	1060	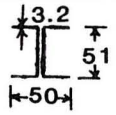	6.33
2	1095	1060	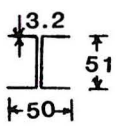	6.44
3	1172	1137	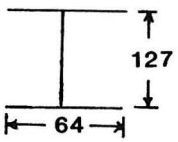	3.24

* centre line to centre line dimensions